

FAST TRANSIENT STABILITY SOLUTIONS

H. W. Dommel N. Sato

Bonneville Power Administration
Portland, Oregon

ABSTRACT

Techniques are described for improving the speed of large transient stability studies without sacrificing accuracy. A fast iterative method for solving the algebraic network equations, including the effect of generator saliency, is explained. A new technique for solving the differential equations with the implicit trapezoidal rule of integration is introduced. These two techniques can be combined into one simultaneous solution, thereby eliminating the problem of interface error between the differential and algebraic equation solutions of the traditional approach.

INTRODUCTION

Transient stability studies now require considerable computer time, especially for solving large systems. This has motivated a search for faster solution techniques. Two possibilities for improving the speed of transient stability studies are: (a) Reduction of the total system to a smaller one, which could be solved faster, and (b) improvements in the numerical solution techniques.

Reduction techniques produce equivalents which are normally only approximations. Therefore, in spite of recent progress in finding equivalents, the user must have a "feeling" for the problem when equivalents are used. It should also be noted that solutions based on sparsity techniques become faster through reduction only to a certain point because of fill-in caused by the reduction process¹. Judicious use of equivalents can make stability solutions faster; however, this paper is concerned with the second possibility, improved numerical solution techniques.

Improvements in numerical solution techniques can speed up the solution without placing any burden of judgment on the user. This paper describes experiments carried out at Bonneville Power Administration (BPA) over the last few years with the objective of obtaining faster solutions for the steady-state equations as well as for the differential equations which arise in stability studies. Speeding up the solution of the steady-state equations has been accomplished by applying sparsity techniques and solution methods which require fewer iterations. Speeding up the solution of the differential equations has been achieved with the implicit trapezoidal rule of integration, which has already been used successfully for the solution of switching transients at BPA². This method is numerically stable and accurate enough. It should be noted that explicit techniques, including the Runge-Kutta methods, require higher accuracy primarily to insure numerical stability. As a consequence, such techniques also require longer solution times. It is expected that implementation of these ideas into BPA's production program will make the solution about five times faster.

Brackets are used to indicate vector and matrix quantities. Parentheses usually indicate a functional relationship or the value for time t . A super dot is used to indicate derivatives with respect to time.

STRUCTURE OF TRANSIENT STABILITY EQUATIONS

The initial conditions for a stability study are determined by a steady-state power flow solution. Thereafter, two sets of equations must be solved simultaneously as a function of time, namely a system

of steady-state equations (which describe the steady-state behavior of the network including steady-state models of loads and the algebraic equations of synchronous machines),

$$\begin{aligned} g_1(x_1, \dots, x_n, y_1, \dots, y_m) &= 0 \\ &\dots\dots\dots \\ g_n(x_1, \dots, x_n, y_1, \dots, y_m) &= 0 \end{aligned} \quad (1)$$

or $[g([x],[y])] = 0$

and a system of differential equations (which describe the dynamic behavior of the machines and their control circuits),

$$\begin{aligned} \dot{y}_1 &= f_1(x_1, \dots, x_n, y_1, \dots, y_m, t) \\ &\dots\dots\dots \text{or } [\dot{y}] = [f([x],[y], t)] \quad (2) \\ \dot{y}_m &= f_m(x_1, \dots, x_n, y_1, \dots, y_m, t) \end{aligned}$$

The structure of Eq. (1) will change at certain moments in time due to fault initialization, fault clearing, line switching, etc. Such changes, which require re-solutions without advancing the time, produce discontinuities in the value of the vector $[x]$. No discontinuities can appear in $[y]$.

CLASSIFICATION OF SOLUTION METHODS

On a digital computer, the values of $[x]$ and $[y]$ are computed at discrete points in time, thereby producing a sequence of snapshot pictures at intervals Δt . The sampling rate $1/\Delta t$ determines the upper limit of the frequencies which will be adequately represented in $[x]$ and $[y]$. As a consequence of the discretization, interpolation assumptions must normally be made on $[x]$ to define the state between discrete points. In most cases linear interpolation is adequate.

The methods for solving Eqs. (1) and (2) simultaneously fall roughly into three categories: (a) Alternating solution of Eqs. (1) and (2), (b) elimination of $[x]$, and (c) algebraization of Eq. (2) by implicit integration. The distinction is not always clear. As an example, the numerical solution of differential equations is in itself based on an algebraization process.

(a) Alternating Solution Method

This technique is probably used in most existing stability programs. The algorithm is roughly as follows:

1. Establish initial conditions by solving Eq. (1) at $t = 0$.
2. Predict how $[x]$ behaves over the next time interval by using zero, first or second order extrapolation.
3. Solve Eq. (2) for $[y(t)]$ by any numerical technique, using the polynomial obtained in step 2 as an interpolation formula.
4. Solve Eq. (1) for $[x(t)]$ by any of the well-known power flow solution techniques.

Paper T72 137-3, recommended and approved by the Power System Engineering Committee of the IEEE Power Engineering Society for presentation at the IEEE Winter Meeting, New York, N.Y., January 30-February 4, 1972. Manuscript submitted September 20, 1971; made available for printing November 19, 1971.

5. Use the computed value $[x(t)]$ to correct the prediction over the interval from $t-\Delta t$ to t .
6. Solve Eq. (2) for $[y(t)]$ by any numerical technique, using the polynomial obtained in step 5 as an interpolation formula.
7. Check differences of two successive solutions for $[y(t)]$. If the differences are negligible proceed to step 8. Otherwise go to step 4.
8. Advance by one time step and loop back to step 2.

Several variations are possible. In the version described above, the steady-state equations (1) must be solved once, most of the time, since the differences in step 7 are normally sufficiently small on the first pass. The prediction and correction process of the alternating solution method should not be confused with predictor-corrector methods for solving differential equations; if such methods are used, steps 3 and 6 would also involve another kind of prediction-correction process in itself.

It is essential to include the check of step 7 to avoid so-called "interface" errors. If this is not done, a careful assessment should be made about the acceptability of the accumulated errors. With the interface loop closed, the quality of the prediction (step 2) will determine how often the loop must be executed and, in effect, how long the study will take, but it will not degrade the accuracy of the solution because of corrections initiated in step 7. This is not true for open-loop solutions, where the quality of the prediction will have a decisive influence on the accuracy.

(b) Elimination of $[x]$

This approach is used for small disturbance stability studies³. For small variations $[\Delta x]$, $[\Delta y]$ around an operating point, Eq. (1) can be linearized,

$$\begin{bmatrix} \frac{\partial g}{\partial x} \\ \frac{\partial g}{\partial y} \end{bmatrix} \begin{bmatrix} \Delta x \\ \Delta y \end{bmatrix} = 0$$

with the Jacobian matrices $\begin{bmatrix} \frac{\partial g}{\partial x} \\ \frac{\partial g}{\partial y} \end{bmatrix}$ being evaluated at the given solution point. Eq. (2) can also be linearized around the operating point,

$$[\Delta \dot{y}] = [A][\Delta y] + [B][\Delta x]$$

Both linear equations combined become

$$\begin{bmatrix} \frac{\partial g}{\partial x} & \frac{\partial g}{\partial y} \\ [B] & [A] \end{bmatrix} \begin{bmatrix} \Delta x \\ \Delta y \end{bmatrix} = \begin{bmatrix} 0 \\ [\Delta \dot{y}] \end{bmatrix}$$

and after elimination of $[x]$ by triangularization,

$$\begin{bmatrix} 0 & & \\ & [A]_{\text{reduced}} & \\ & & \end{bmatrix} \begin{bmatrix} \Delta x \\ \Delta y \end{bmatrix} = \begin{bmatrix} 0 \\ [\Delta \dot{y}] \end{bmatrix}$$

or

$$[\Delta \dot{y}] = [A]_{\text{reduced}} [\Delta y] \quad (3)$$

The eigenvalues of $[A]_{\text{reduced}}$ give the damping (real part) and natural frequencies (imaginary part) of all possible modes of oscillations without having to make any assumption about the specific (small) disturbance. The system will be stable as long as the real parts of all eigenvalues are negative (first method of Lyapunov).

(c) Algebraization by Implicit Integration

The step-by-step solution of Eq. (2) is best expressed in integral form,

$$[y(t)] = [y(t-\Delta t)] + \int_{t-\Delta t}^t [f([y],[x],\tau)] d\tau$$

Implicit integration techniques use interpolation functions for the expressions under the integral. Interpolation means that the functions must pass through the yet unknown points at time t , which must therefore be expressed as variables. In general, the solution may require iterations. If the differential equations are linear, however, then a direct solution becomes possible.

Let the differential equations (2) be linear of the form

$$[\dot{y}] = [A][y] + [B][x] \quad (4a)$$

Most differential equations are linear in stability studies. There are some nonlinearities, however, but their inclusion poses no serious problem, as shown later for the excitation system. Eq. (4a) can be rewritten as a step-by-step integration,

$$[y(t)] = [y(t-\Delta t)] + [A] \int_{t-\Delta t}^t [y] d\tau + [B] \int_{t-\Delta t}^t [x] d\tau \quad (4b)$$

The simplest implicit integration scheme is the trapezoidal rule of integration.* It is based on the assumption that $[x]$ and $[y]$ vary linearly over the interval from $t-\Delta t$ to t . Then Eq. (4b) becomes

$$[y(t)] = [y(t-\Delta t)] + \frac{\Delta t}{2} [A] \left[[y(t-\Delta t)] + [y(t)] \right] + \frac{\Delta t}{2} [B] \left[[x(t-\Delta t)] + [x(t)] \right]$$

which is simply a system of linear algebraic equations

$$\left[[U] - \frac{\Delta t}{2} [A] \right] [y(t)] - \frac{\Delta t}{2} [B] [x(t)] = [c(t-\Delta t)] \quad (5a)$$

The vector on the right-hand side is known from the values already computed at the preceding time step:

$$[c(t-\Delta t)] = \frac{\Delta t}{2} [B] [x(t-\Delta t)] + \left[[U] + \frac{\Delta t}{2} [A] \right] [y(t-\Delta t)] \quad (5b)$$

$[U]$ denotes the unit or identity matrix. Eq. (5a) can now be solved directly with Eq. (1) as one complete system of steady-state equations.

NUMERICAL STABILITY OF THE TRAPEZOIDAL RULE OF INTEGRATION

The trapezoidal rule of integration is numerically stable. To illustrate the problem of numerical stability, it will be assumed that a fast oscillation in a control circuit produces "ripples" of very small magnitudes which do not have any influence on the overall behavior of the circuit. Such a mode of oscillation could be described by

$$\ddot{y} + y = 0, \text{ with } y(0) = 0, \dot{y}(0) = 10^{-4} \quad (6a)$$

The exact solution for this ripple is $y = 10^{-4} \sin(t)$; its amplitude of 10^{-4} will be considered as very small by definition. Eq. (6a) must be rewritten as a system of first-order differential equations in order to apply any of the numerical solution techniques:

$$\begin{bmatrix} \dot{y}_1 \\ \dot{y}_2 \end{bmatrix} = \begin{bmatrix} 0 & 1 \\ -1 & 0 \end{bmatrix} \begin{bmatrix} y_1 \\ y_2 \end{bmatrix} \text{ with } \begin{matrix} y_1 = y \\ y_2 = \dot{y} \end{matrix} \quad (6b)$$

The exact step-by-step solution is

$$\begin{bmatrix} y_1(t) \\ y_2(t) \end{bmatrix} = e^{[A]\Delta t} \begin{bmatrix} y_1(t-\Delta t) \\ y_2(t-\Delta t) \end{bmatrix} \text{ whereby } [A] = \begin{bmatrix} 0 & 1 \\ -1 & 0 \end{bmatrix}$$

with the transition matrix $e^{[A]\Delta t}$. Application of the trapezoidal rule to Eq. (6b) gives

$$\begin{bmatrix} y_1(t) \\ y_2(t) \end{bmatrix} = \frac{1}{1 + \frac{\Delta t^2}{4}} \begin{bmatrix} 1 - \frac{\Delta t^2}{4} & \Delta t \\ -\Delta t & 1 - \frac{\Delta t^2}{4} \end{bmatrix} \begin{bmatrix} y_1(t-\Delta t) \\ y_2(t-\Delta t) \end{bmatrix} \quad (7)$$

* There are also higher-order generalizations of the trapezoidal rule⁴.

It can be shown that $y_1^2(t) + y_2^2(t) = y_1^2(t-\Delta t) + y_2^2(t-\Delta t)$ in Eq. (7) for any choice of Δt . Therefore, if the process is started with the correct initial condition $y_1^2(0) + y_2^2(0) = 10^{-8}$, the solution for y will always lie between -10^{-4} and $+10^{-4}$, even for step-widths which are much larger than one cycle of the oscillation. In other words, the trapezoidal rule "cuts across" oscillations which are very fast but of negligible amplitude, without any danger of numerical instability.

Explicit integration techniques, which include Runge-Kutta methods, are inherently unstable. They require a step-width tailored to the highest frequency or smallest time constant (rule of thumb: $\Delta t \leq \frac{1}{5} T_{\min}$) even though this mode may produce only negligible ripples, with the overall behavior determined by large time constants, as in so-called "stiff-systems."

Applying the conventional fourth-order Runge-Kutta method to Eq. (6b) is identical to a fourth-order Taylor series expansion of the transition matrix in case of linear systems,

$$e^{[A]\Delta t} \cong [U] + \Delta t[A] + \frac{\Delta t^2}{2}[A]^2 + \frac{\Delta t^3}{6}[A]^3 + \frac{\Delta t^4}{24}[A]^4.$$

Adding the 5 terms gives

$$\begin{bmatrix} y_1(t) \\ y_2(t) \end{bmatrix} = \begin{bmatrix} 1 - \frac{\Delta t^2}{2} + \frac{\Delta t^4}{24} & \Delta t - \frac{\Delta t^3}{6} \\ -\Delta t + \frac{\Delta t^3}{6} & 1 - \frac{\Delta t^2}{2} + \frac{\Delta t^4}{24} \end{bmatrix} \cdot \begin{bmatrix} y_1(t-\Delta t) \\ y_2(t-\Delta t) \end{bmatrix} \quad (8)$$

Plotting the curves with a reasonably small Δt , e.g., 6 samples/cycle, reveals that the Runge-Kutta method of Eq. (8) is more accurate at first than the trapezoidal rule, but tends to lose the amplitude later on (Fig. 1).

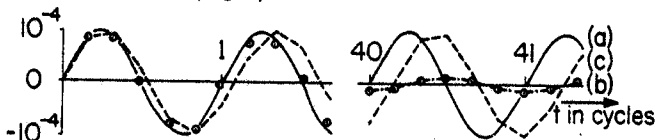


Fig. 1. Numerical solution of $\ddot{y} + y = 0$
(a) Exact, (b) Runge-Kutta,
(c) trapezoidal rule

This is not serious since the ripple is assumed to be unimportant in the first place. If the step-width is increased, however, to $\Delta t > \frac{\sqrt{2}}{\pi}$ cycles ($\Delta t > 0.4502$ cycles), then the amplitude will eventually grow to infinity. This is illustrated in table I for $\Delta t = 1$ cycle.

Table I. Numerical solution of Eq. (6a) with $\Delta t = 1$ cycle

t in cycles	1	2	3	4	5	6
exact	0	0	0	0	0	0
trapezoidal rule	$0.58 \cdot 10^{-4}$	$-0.94 \cdot 10^{-4}$	$0.96 \cdot 10^{-4}$	$-0.63 \cdot 10^{-4}$	$0.06 \cdot 10^{-4}$	$0.53 \cdot 10^{-4}$
Runge-Kutta	-0.004	-0.32	-18	-590	6800	2,600,000

VERY SMALL TIME CONSTANTS IN THE TRAPEZOIDAL RULE

The fact that the trapezoidal rule of integration is stable even if the step-width is much larger than the smallest time constant is of practical importance for stability studies. Fig. (2a) shows a hypothetical control circuit with a smallest time constant of 0.0001 s, and a step function input, which is regarded as the most severe test.

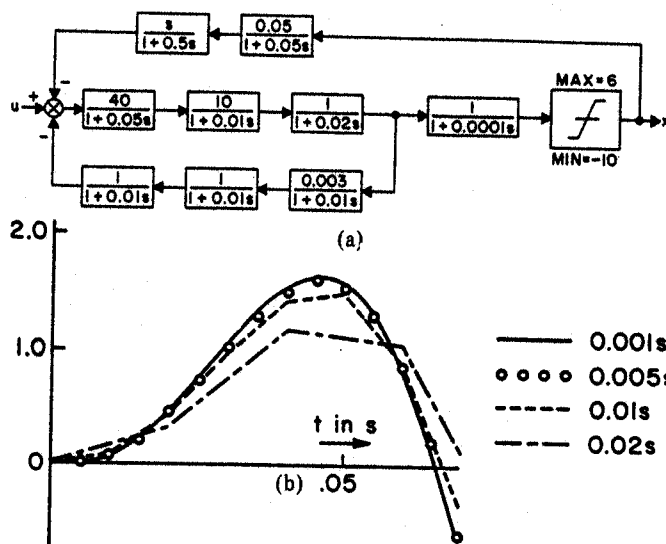


Fig. 2. Test example for trapezoidal rule.
(a) Control circuit. (b) Solution for step-function input $u = 0.2$.

The plots of Fig. (2b) were obtained with the trapezoidal rule, using different step-widths. The results are acceptable with a step-width as large as 0.01 s, which is 500 times larger than the approximate step-width $\frac{1}{5} T_{\min}$ required for the Runge-Kutta method.

Block diagrams with small time constants are often described by equations of the form

$$T \frac{dy_2}{dt} = Ky_1 - y_2, \quad (9)$$

as in Fig. (2a). If T is very small, then the block is basically a multiplier,

$$y_2 = Ky_1 \quad \text{if } T \cong 0 \quad (10)$$

If explicit integration techniques are used in such cases, then it becomes necessary to set small time constants equal to zero to avoid numerical instability. This is bothersome to the user because the problem manifests itself quite often only after the algorithm has failed to give a solution. On the other hand, the programmer hesitates to build the decision into the program because it is difficult to draw the line between small and not so small time constants for all possible situations. This problem does not arise with the trapezoidal rule since

the limit case $T=0$ turns out to be identical to the algebraic equation (10). Applying the trapezoidal rule to Eq. (9) gives

$$\left(1 + \frac{2T}{\Delta t}\right) y_2(t) - Ky_1(t) = -\left(1 - \frac{2T}{\Delta t}\right) y_2(t-\Delta t) + Ky_1(t-\Delta t)$$

and for $T \ll \Delta t$

$$y_2(t) - Ky_1(t) = -\left(y_2(t-\Delta t) - Ky_1(t-\Delta t)\right), \quad (11)$$

which is indeed identical to Eq. (10) as long as the process starts from the correct initial conditions $y_2(0) - Ky_1(0) = 0$. Even a slight error in the initial conditions,

$$y_2(0) - Ky_1(0) = \epsilon$$

will not cause serious problems. Since Eq. (11) just flips the sign of the expression $y_2 - Ky_1$ from step to step, the error ϵ would only produce ripples $\pm \epsilon$ superimposed on the true solution for y_2 . These ripples will disappear entirely when y_2 passes through another trapezoidal integration.

FAST SOLUTION OF THE STEADY-STATE EQUATIONS

The steady-state equations in stability studies differ very little from those used in conventional power flow studies, except that the real and reactive power of loads become voltage dependent and more steady-state equations are added for the synchronous generators. On the other hand, some features in power flow studies, such as automatic tap setting of transformers, are not required in stability studies.

Generator Model

A generator model with three armature windings, one field winding and one hypothetical g-coil (which represents deeper flowing eddy currents in steam generators), is adequate to represent transient effects (subtransient effects ignored). The additional steady-state equations for this model are *):

$$\begin{bmatrix} I_q \\ I_d \end{bmatrix} = \frac{1}{R_a^2 + X_d' X_q'} \begin{bmatrix} R_a & X_d' \\ -X_q' & R_a \end{bmatrix} \begin{bmatrix} E_q' - V_q \\ E_d' - V_d \end{bmatrix} \quad (12)$$

with the quantities in the q, d-reference frame related to the phasor quantities \bar{I} , \bar{V} , \bar{E}' of the network solution by

$$I_q + jI_d = \bar{I} \cdot e^{j\delta}, \text{ with } \bar{I} = I_{\text{real}} + jI_{\text{imag}}, \text{ analogous for } \bar{V}, \bar{E}' \quad (13)$$

The angle δ measures the rotor position of the generator relative to the synchronously rotating reference frame, which is implied in phasor solutions of the network. The parameters δ , E_q' , E_d' are part of the vector $[y]$, whose value is determined from the solution of the differential equations, whereas I_q , I_d , V_q , V_d are part of the vector $[x]$. In the alternating solution method, δ , E_q' , E_d' are treated as known quantities during the solution of the steady-state equations.

Eq. (12) is easy to handle if saliency is ignored, that is, if $X_q' = X_d'$. In this case, the 2 equations can be written as one equation with phasor quantities,

$$\bar{I} = \frac{1}{R_a + jX_d'} (\bar{E}' - \bar{V}) \text{ for } X_q' = X_d' \quad (14)$$

which is simply a known voltage \bar{E}' behind transient impedance $R_a + jX_d'$. In effect, each internal node with the voltage \bar{E}' is a slack node.

The inclusion of Eq. (12) in the network solution becomes more complicated if saliency is considered, that is, if $X_q' \neq X_d'$. When Eq. (12) is transformed to the reference frame of the network solution,

$$\begin{bmatrix} I_{\text{real}} \\ I_{\text{imag}} \end{bmatrix} = [M(t)] \begin{bmatrix} E'_{\text{real}} - V_{\text{real}} \\ E'_{\text{imag}} - V_{\text{imag}} \end{bmatrix}, \quad (15)$$

*): The newly recommended position for the quadrature axis lagging 90° behind the direct axis is adopted.⁷

$$\text{with } [M(t)] = \frac{1}{R_a^2 + X_d' X_q'} \begin{bmatrix} \cos\delta - \sin\delta & [R_a \ X_d'] \\ \sin\delta \cos\delta & [-X_q' \ R_a] \end{bmatrix} \begin{bmatrix} \cos\delta & \sin\delta \\ \sin\delta & \cos\delta \end{bmatrix}$$

then two complications in Eq. (15) as compared to Eq. (14) become apparent:

1. It is no longer possible to combine the two equations (15) into one phasor equation, and
2. the matrix $[M(t)]$ is now a function of time, with δ entering into it.

If subtransient effects are to be included, then the model must have two more windings "kd" and "kq" in the direct and quadrature axis to represent damper bars or hypothetical coils for surface eddy currents. This adds 2 more differential equations, but the algebraic equations can again be reduced to the form of Eq. (12) except that the primed quantities are now replaced by double primed quantities,

$$\begin{bmatrix} I_q \\ I_d \end{bmatrix} = \frac{1}{R_a^2 + X_d'' X_q''} \begin{bmatrix} R_a & X_d'' \\ -X_q'' & R_a \end{bmatrix} \begin{bmatrix} E_q'' - V_q \\ E_d'' - V_d \end{bmatrix} \quad (16)$$

All arguments for the model with transient effects are, therefore, also applicable to the model including subtransient effects.

The complete system of steady-state equations is solved by adopting well-known techniques for fast power flow solutions to the stability problem. The improvement in the solution of systems of linear equations by optimally ordered triangular factorization with the sparsity of the matrix exploited^{5,6} has eliminated the Gauss-Seidel iterative method (using the admittance matrix) as a serious contender, leaving only two competitive techniques: (a) the iterative method using the triangularized admittance matrix and (b) Newton-Raphson method.

(a) Iterations with the Triangularized Admittance Matrix

First, the inclusion of Eq. (12) or (16) must be resolved. The simplest way would be to use the terminal current $I_{\text{real}} + jI_{\text{imag}}$ as a given node current and adjust it iteratively as improved answers are obtained for $V_{\text{real}} + jV_{\text{imag}}$. Experiments have shown, however, that this simple technique fails to converge quite frequently. Convergence can be improved considerably by creating a fictitious slack node behind an impedance; the value of the slack node voltage will then depend more or less on $V_{\text{real}} + jV_{\text{imag}}$ and must, therefore, be adjusted iteratively. Using $R_a + jX_d'$ as the impedance to the fictitious slack node improves the situation, but in some cases convergence is still difficult.

It was found that the convergence becomes very fast if the admittance to the fictitious slack node is set to

$$\bar{Y}_{\text{fictitious}} = \frac{R_a - j \frac{1}{2} (X_d' + X_q')}{R_a^2 + X_d' X_q'}$$

Two or three iterations are normally sufficient to adjust the fictitious slack node voltage, or-if an equivalent current source is used in parallel with the shunt admittance $\bar{Y}_{\text{fictitious}}$ instead of a voltage source, as in BPA's stability program (Fig. 3)-to adjust the fictitious current source.

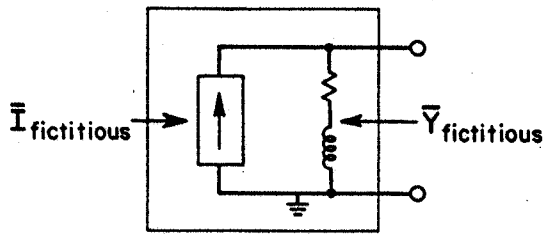


Fig. 3. Equivalent circuit for generator.

The value of the current source is determined from

$$\bar{I}_{\text{fictitious}} = \frac{R_a - j\frac{1}{2}(X_d' + X_q')}{R_a^2 + X_d'X_q'} \cdot \bar{E}' + \bar{I}_{\text{saliency}} \quad (17a)$$

with the first part being known and the second part being adjusted iteratively:

$$\bar{I}_{\text{saliency}} = -j\frac{1}{2} \frac{X_q' - X_d'}{R_a^2 + X_d'X_q'} (\bar{E}'^* - \bar{V}^*) e^{j2\delta} \quad (17b)$$

(all quantities are phasors in the network solution reference frame; "*" denotes conjugate complex). As an initial guess for the terminal voltages, the values obtained at the preceding time step are used, except that their angle is advanced by the same amount by which the internal angle δ has changed from $t-\Delta t$ to t . Omitting this rotation would double the number of required iteration steps.

Techniques for avoiding the iterations due to saliency altogether are hardly worthwhile, because these 2 or 3 iterations do not add to the number of iterations which are normally required for non-impedance load models anyhow. Also, gains in one place would probably be offset somewhere else (example: If two real equations with two real variables were used on terminal nodes of generators, then Eq. (15) could be used without any need for iterations. However, the admittance matrix would then have to be partly triangularized in each time step because of the time-dependence of $[M]$).

The nodes can now be subdivided into two sets,

- subset 1 of all "external" nodes (terminals of generators, loads, passive nodes) and,
- subset 2 of all "internal" nodes (true slack nodes if $X_q' = X_d'$, fictitious slack nodes otherwise).

The nodal admittance matrix is partitioned accordingly,

$$[\bar{Y}] = \begin{bmatrix} [\bar{Y}_{11}] & [\bar{Y}_{12}] \\ [\bar{Y}_{21}] & [\bar{Y}_{22}] \end{bmatrix}$$

With $[\bar{V}_2]$ known (slack bus voltages), $[\bar{V}_1]$ has to be found by solving the system of linear equations,

$$[\bar{Y}_{11}][\bar{V}_1] = [\bar{I}_1] - [\bar{Y}_{12}][\bar{V}_2] \quad (18)$$

All other quantities can then be computed from $[\bar{V}_1]$ and $[\bar{V}_2]$. Eq. (18) is solved by triangular factorization, using optimal ordering and sparsity techniques. The matrix $[\bar{Y}_{11}]$ must only be triangularized initially and whenever network changes (short-circuit, line switchings) take place. Otherwise, it remains constant for all iteration steps as well as over the time steps. With $[\bar{Y}_{11}]$ already triangularized, Eq. (18) is solved by a "repeat" solution, in which the triangularization process is extended to the right-hand side only. Repeat solutions are

* Loads which cannot be modeled as constant impedance.

about five times faster than triangularization of the matrix. Typical solution times on a CDC 6400 for a 1190-node case are:

Triangular factorization of the matrix	8.6 s
repeat solution	1.6 s

The term $[\bar{Y}_{12}][\bar{V}_2]$ in Eq. (18) is identical with the generator currents from Eq. (17a), with $\bar{I}_{\text{saliency}} = 0$ if $X_q' = X_d'$. The vector $[\bar{I}_1]$ represents the current injections on the external nodes, including load nodes. Loads are converted to equivalent impedances which give the correct power at the nominal voltages of the initial power flow solution; their values enter into the diagonal elements of $[\bar{Y}_{11}]$. If all loads are represented as impedances then Eq. (18) would be non-iterative with $[\bar{I}_1] = 0$, except for iterations due to saliency. If loads are not modeled as constant impedances, then $[\bar{I}_1]$ is adjusted iteratively to account for the difference between quadratic voltage dependence of the impedance and the specified voltage dependence. Converting the loads to impedances at nominal voltage reduces the number of iterations by one half as compared to representing the loads entirely in $[\bar{I}_1]$. The average number of iterations depends very much on the load representations; 5 to 7 iterations are typical figures. Unrealistic load representations may increase the number of iterations appreciably. The user should have good reason, therefore, to represent loads which differ appreciably from constant impedance.

(b) Newton-Raphson Method

The Newton-Raphson method applied to Eq. (18) has already been explained in detail elsewhere^{8,9}; therefore, the equations will not be repeated here. The most promising approach with the Newton-Raphson method is the version which uses the current equation form and rectangular coordinates for the variables⁹, with the following modification: Re-use the old Jacobian matrix from the preceding time step for the first iteration step (this requires saving the lower as well as the upper triangular matrix, though) and compute a new Jacobian matrix for the next iteration step. These two steps (one repeat solution plus one complete solution) usually solve the steady-state equations with sufficient accuracy. The version using the current equation and rectangular coordinates has the advantage of being non-iterative for nodes with constant impedance loads⁹. Saliency does not pose any problem because 2N real equations and variables are used in the Newton-Raphson method anyhow, instead of N complex equations and variables, and because the matrix must be triangularized anew in each time step. In this case, Eq. (15) is easy to handle because it is linear in the unknown variables V_{real} and V_{imag} .

(c) Comparison of the Two Methods

The iterative solution using the triangularized admittance matrix and the Newton-Raphson method are closely competitive. At this time, the former method appears to be faster and preferable for the following reasons:

1. The Newton-Raphson method requires one re-triangularization in each time step, whereas the admittance matrix must only be re-triangularized when network changes take place. Tests indicate that the solution with the triangularized admittance matrix is faster if it converges in less than 5 to 10 iterations.
2. The Newton-Raphson method requires more storage, up to three times as much when the lower triangular matrix is saved.

In the second argument it was assumed that the matrix $[\bar{Y}_{11}]$ is symmetric; the lower triangular matrix is not needed then. The comparison becomes less advantageous for the triangularized admittance matrix if the network contains phase shifting transformers. In

such cases, those columns of the lower triangular matrix which are affected by the phase-shifting transformers must also be stored.

It is entirely possible that the problem formulation will change in future stability studies in such a way that the Newton-Raphson method will become preferable. One situation which is difficult to handle with the triangularized admittance matrix, but is very easy with the Newton-Raphson method, is the node type where real power and voltage magnitude are specified. Another situation which might be easier with the Newton-Raphson method is frequency-dependence of machines, of loads, and line impedances.

SIMULTANEOUS SOLUTION OF STEADY-STATE AND DIFFERENTIAL EQUATIONS

The feasibility of speeding up stability studies by using the trapezoidal rule of implicit integration has been demonstrated at BPA with a number of test cases. These experiments will be explained in order of increasing complexity.

Swing Equation

The only differential equations in "classical" stability studies are the swing equations for each generator:

$$(\omega J) \frac{d\omega}{dt} = P_m - P_{el} \quad (19)$$

$$\text{and} \quad \frac{d\delta}{dt} = \omega - \omega_s \quad (20)$$

with J = moment of inertia,

ωJ = angular momentum,

ω = speed (ω_s = synchronous speed) on electrical side,

δ = rotor position relative to synchronously rotating reference frame,

P_m = shaft power input,

P_{el} = electrical power output, corrected for electrical losses.

For simplicity, damping terms will be neglected in Eq. (19), but their inclusion poses no serious problem. It is also customary to set $\omega J \approx \omega_s J$, which is permissible as long as the speed deviates very little from the synchronous speed. In other cases, ωJ should be changed as the speed changes.

Since classical stability studies have been performed for many years, long before digital computers became available, it is worthwhile to look at the techniques which were used for hand calculations. The most frequently used procedure has been a predictor formula¹⁰:

$$\delta(t) = 2\delta(t-\Delta t) - \delta(t-2\Delta t) + \frac{(\Delta t)^2}{\omega(t-\Delta t)J} (P_m - P_{el}(t-\Delta t)) \quad (21)$$

Eq. (21) can be derived by making two assumptions:

1. Integrate Eq. (19) from midpoint $t - \frac{3}{2}\Delta t$ to midpoint $t - \frac{1}{2}\Delta t$, assuming that $\frac{P}{\omega}$ varies linearly in this interval, which gives

$$\omega(t - \frac{1}{2}\Delta t) = \omega(t - \frac{3}{2}\Delta t) + \frac{\Delta t}{\omega(t - \Delta t)J} (P_m - P_{el}(t-\Delta t))$$

2. Integrate Eq. (20) from $t - \Delta t$ to t , assuming that ω varies linearly in this interval with its average value being $\omega(t - \frac{1}{2}\Delta t)$.

Eq. (21) is sufficiently accurate for normal step-widths of 1 to 5 cycles. There is no reason, therefore, why it should not be used in computer programs, especially if a corrector formula is added as a safeguard.

The corrector formula is easily obtained by applying the trapezoidal rule to Eq. (19) and (20), which gives

$$\delta(t) = -\frac{(\Delta t)^2}{4(\omega J)} P_{el}(t) + \alpha(t-\Delta t) \quad (22a)$$

with $\alpha(t-\Delta t)$ being known from values at the preceding time step,

$$\alpha(t-\Delta t) = \delta(t-\Delta t) + \Delta t \left(\omega(t-\Delta t) - \omega_s \right) + \frac{(\Delta t)^2}{4(\omega J)} \left(2P_m - P_{el}(t-\Delta t) \right) \quad (22b)$$

In Eq. (22) it is assumed that P_m is constant, but the equation can easily be changed if P_m changes as a function of time or if the torque T_m is constant.

Eq. (22a) must be used after discontinuities where Eq. (21) is no longer valid and should be used at other times to avoid interface errors. It is merged into the solution of the steady-state equations as follows:

1. Predict δ with Eq. (21) (at times of discontinuities assume that δ will not change over the next interval).
2. At the end of each steady-state iteration step (or in the back-substitution) compute P_{el} and insert it into Eq. (22a) to get a corrected angle. Correct the angle only if the change is noticeable, to avoid unnecessary computations of $\sin \delta$ and $\cos \delta$.
3. Update α after the steady-state solution has been completed.

A more direct approach could be used with the Newton-Raphson method, where Eq. (22a) could be added as an additional equation and δ as an additional variable. The size of the Jacobian matrix would not increase if δ is eliminated as soon as the elimination hits the rows of the terminal node, that is, if the technique is used which was described for phase shifting angles in reference 9.

Except at times of discontinuities, the corrections are normally quite small, and in such cases, Eq. (22a) serves only as a check. If iterations are required anyhow because of saliency or non-impedance loads, then the corrector formula Eq. (22) will not add to the total number of iterations.

Differential Equations of the Generator

For a generator model with transient effects only, there are two differential equations,

$$\frac{dE'_q}{dt} = -\frac{1}{T'_{do}} \left(E'_q - (X_d - X'_d) I_d - E_{FD} \right) \quad (23a)$$

$$\frac{dE'_d}{dt} = -\frac{1}{T'_{qo}} \left(E'_d + (X_q - X'_q) I_q \right) \quad (23b)$$

(E_{FD} = voltage applied to terminals of field winding). Application of the trapezoidal rule transforms Eq. (23) into

$$E'_q(t) = a_d(X_d - X'_d) I_d(t) + F_q \quad (24a)$$

$$E'_d(t) = -a_q(X_q - X'_q) I_q(t) + F_d \quad (24b)$$

with F_q and F_d being known from values at the preceding time step at $t-\Delta t$ and from $E_{FD}(t)$ (which is also known if the exciter is represented as a simple voltage source),

$$F_q = E'_q(t-\Delta t) + a_d \left(E_{FD}(t-\Delta t) + E_{FD}(t) - 2E'_q(t-\Delta t) + (X_d - X'_d) I_d(t-\Delta t) \right) \quad (25a)$$

$$F_d = E_d'(t-\Delta t) - a_q \left(2E_d'(t-\Delta t) + (X_q - X_q') I_q(t-\Delta t) \right) \quad (25b)$$

with
$$a_d = \frac{\Delta t}{\Delta t + 2T_{do}'}, \quad a_q = \frac{\Delta t}{\Delta t + 2T_{qo}'}$$

Eq. (24) inserted into Eq. (12) gives the complete description of all algebraic and differential equations, reduced to an equivalent of two algebraic equations:

$$\begin{bmatrix} I_q \\ I_d \end{bmatrix} = \frac{1}{R_a^2 + X_{dmod}' X_{qmod}'} \begin{bmatrix} R_a & X_{dmod}' \\ -X_{qmod}' & R_a \end{bmatrix} \begin{bmatrix} F_q & -V_q \\ F_d & -V_d \end{bmatrix} \quad (26)$$

with the modified reactances

$$X_{dmod}' = X_d' + a_d (X_d - X_d')$$

$$X_{qmod}' = X_q' + a_q (X_q - X_q')$$

For normal time constants and step-widths in the order of a few cycles, the modified transient reactances differ only by a few percent from the original transient reactances. The only approximation which had to be made is linear interpolation between $t-\Delta t$ and t for the quantities E_q' , E_d' , I_q , I_d , E_{FD} . It is significant that Eq. (26) has the same structure as Eq. (12). As a consequence, Eq. (26) can simply replace Eq. (12) with no need to change the solution algorithm which was already developed for Eq. (12). The differential equations (23) will be solved implicitly without requiring any extra work, except that F_q and F_d have to be updated from step to step. At times of discontinuities with no advance in time, Eq. (12) must be used in place of Eq. (26) for the second "post-change" solution, or, if it is desirable to keep the impedances unchanged, Eq. (26) may be used iteratively with the following values for F_q and F_d :

$$F_q = E_q' - a_d (X_d - X_d') I_d$$

$$F_d = E_d' + a_q (X_q - X_q') I_q$$

with E_q' , E_d' determined from the "pre-change" solution and I_q , I_d being obtained iteratively within the "post-change" solution.

The same ideas should be applicable to generator models which include subtransient effects. In this case, large step-widths (greater than 1-2 cycles) may not be able to represent the fast decay of the currents in the kd- and kq-windings after discontinuities very accurately, but the subsequent oscillations and the over-all damping effect should be fairly accurate. Tests are planned to verify this conjecture.

Excitation System

Inclusion of the excitation system was tried with a 9-bus test example. It contained three generators with their swing equations. Two of them were "classical" generator representations, described by Eq. (14), and one was a fully represented generator, described by Eq. (12) and (23), with an exciter model of type 1 as defined in Ref. 11. The smallest time constant in the exciter model was $T_R = 0.06$ s.

First, the differential equations of the four exciter blocks are transformed into algebraic equations with the trapezoidal rule. These can then be reduced to one linear algebraic equation of the form,

$$E_{FD}(t) = E_o - b V_T(t) \quad (27)$$

and one inequality
$$E_{LOW} \leq E_{FD}(t) \leq E_{HIGH} \quad (28)$$

The saturation is taken into account by linearizing the feedback $S_{E_{FD}}$ around the solution point at the preceding time step at $t-\Delta t$, which gives an equation of the form

$$S_{E_{FD}} = k_1 E_{FD} - k_2 \quad (29)$$

with k_1 and k_2 being known. A simpler way would be to use a piecewise linear saturation curve; in this case, k_1 and k_2 would not have to be reevaluated in each time step but only when a new region of the piecewise linear curve is entered. For the 9-bus test example, a linearized curve with only 2 slopes, one for the unsaturated and one for the saturated region, gave results which were close enough for practical purposes to those obtained with the detailed saturation curve.

The parameter b in Eq. (27) is recomputed whenever k_1 and k_2 change, or whenever the regulator output reaches its limit,

$$b = \frac{K_A/a_R}{a_A a_E + K_F K_A / (T_F + \frac{\Delta t}{2})} \quad (30)$$

with
$$a_R = \frac{2T_R}{\Delta t} + 1, \quad a_A = \frac{2T_A}{\Delta t} + 1, \quad a_E = \frac{2T_E}{\Delta t} + K_E + k_1$$

The value E_o is computed from a linear combination of the values of five state variables (including E_{FD} and V_T) at the preceding time step $t-\Delta t$.

The limits E_{LOW} and E_{HIGH} are dynamic limits and not the steady-state limits of the exciter. They can easily be computed in each time step by assuming that the regulator output V_R goes from its state at $t-\Delta t$ to its upper or lower limit at time t ,

$$E_{HIGH} = (b_E + V_R \text{ MAX})/a_E$$

$$E_{LOW} = (b_E + V_R \text{ MIN})/a_E$$

with
$$b_E = E_{FD}(t-\Delta t) \left(\frac{2T_E}{\Delta t} - K_E - k_1 \right) + V_R(t-\Delta t) + 2k_2.$$

Once the regulator output reaches its limit, the parameter K_A is temporarily set to zero in computing b from Eq. (30), and V_R is set to its limit. Thereafter, the derivative of the regulator output is used to check when to back off the limits again, in which case K_A is restored to its original value.

The inclusion of the excitation system in the solution of the steady-state equations is now very simple:

1. Update the state variables of the exciter at time $t-\Delta t$; compute E_o , b , E_{HIGH} , E_{LOW} and an estimate for $E_{FD}(t)$ with Eq. (27) by assuming that V_T will not change from $t-\Delta t$ to t .
2. At the end of each steady-state iteration, compute $E_{FD}(t)$ from Eq. (27), observing the constraints of Eq. (28), and correct F_q as defined in Eq. (25a) accordingly.

The iterative adjustments of $E_{FD}(t)$ and F_q will not add to the 2-3 iterations required for saliency or to additional iterations caused by non-impedance loads.

It cannot be emphasized strongly enough that the few extra statements in the steady-state solution (two expressions for finding E_{FD} and correcting F_q and two IF-statements for checking the limits of E_{FD}) will implicitly bring about the solution of the differential equations without adding more iterations than are required for saliency and non-impedance loads, and without producing interface errors. The updating formulas are also simple enough to be very fast (35 FORTRAN statements in the test program).

Fig. 4 shows the field voltage E_{FD} using the described technique with step-widths of 1 and 5 cycles (fault applied at $t=0$, fault cleared and line removed at $t=5$ cycles). The larger step-width produces acceptable results without any danger of numerical instability.

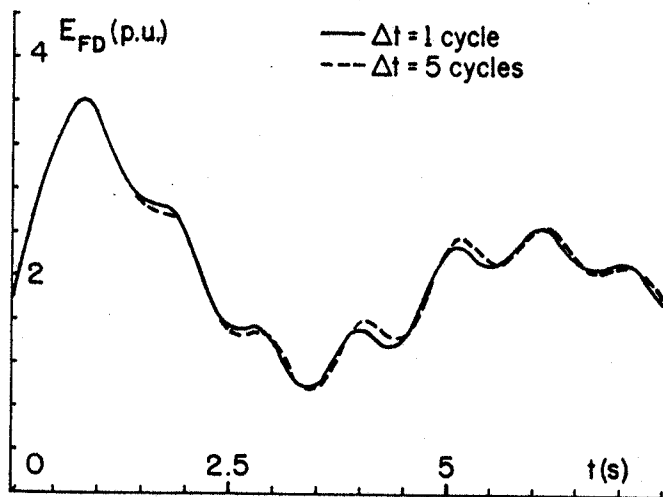


Fig. 4. E_{FD} as function of time.

A more direct approach would be possible with the Newton-Raphson method where an additional equation (27) and an additional variable E_{FD} could be added directly in the same fashion as indicated for the swing equation.

CONCLUSION

In describing the authors' experience in solving transient stability problems, this paper covers two methods in particular which drastically reduce solution times without sacrificing accuracy: (1) Efficient solution of the steady-state network equations using optimally ordered triangular factorization, and special techniques to reduce the number of iterations due to generator saliency and non-impedance loads and (2) Solution of the differential equations with the trapezoidal rule of integration, which is very fast and numerically stable. It also eliminates the interface problem.

ACKNOWLEDGEMENT

The authors are indebted to F. D. Byrnes, Bonneville Power

Administration, for his many contributions, notably for his technique for handling saliency as described in the paper.

REFERENCES

- 1 W. F. Tinney and N. M. Peterson, "Steady-state security monitoring," Brown-Boveri Symposium, Real-Time Control of Electric Power Systems, Baden, Switzerland, Sept. 27-28, 1971.
- 2 H. W. Dommel, "Digital computer solution of electromagnetic transients in single and multiphase networks," IEEE Trans. Power Apparatus and Systems, vol. PAS-88, pp. 388-399, April 1969.
- 3 J. A. Pinnello and J. E. VanNess, "Dynamic response of a large power system to a cyclic load produced by a nuclear accelerator," IEEE Trans. Power Apparatus and Systems, vol. PAS-90, pp. 1856-1862, July/August 1971.
- 4 E. J. Davison, "A high-order Crank-Nicholson technique for solving differential equations," The Computer Journal, vol. 10, no. 2, pp. 195-197, August 1967.
- 5 N. Sato and W. F. Tinney, "Techniques for exploiting the sparsity of the network admittance matrix," IEEE Trans. Power Apparatus and Systems, vol. 82, pp. 944-950, December 1963.
- 6 W. F. Tinney and J. W. Walker, "Direct solutions of sparse network equations by optimally ordered triangular factorization," Proc. IEEE, vol. 55, pp. 1801-1809, November 1967.
- 7 IEEE Committee Report, "Recommended phasor diagram for synchronous machines," IEEE Trans. Power Apparatus and Systems, vol. PAS-88, pp. 1593-1610, November 1969.
- 8 W. F. Tinney and C. E. Hart, "Power flow solution by Newton's method," IEEE Trans. Power Apparatus and Systems, vol. PAS-86, pp. 1449-1460, November 1967.
- 9 H. W. Dommel, W. F. Tinney, and W. L. Powell, "Further developments in Newton's method for power system applications," IEEE Paper No. 70 CP 161 - PWR, presented at the IEEE Winter Power Meeting, New York, Jan. 25-30, 1970.
- 10 O. G. C. Dahl, Electric Power Circuits, vol. II, Power System Stability. New York: Mc-Graw Hill, 1938, pp. 391-401.
- 11 IEEE Committee Report, "Computer representation of excitation systems," IEEE Trans. Power Apparatus and Systems, vol. PAS-87, pp. 1460-1464, June 1968.